CHEMISTRY OF MATERIALS

COMMUNICATION

pubs.acs.org/cm

$SrHfO_3$ Films Grown on Si(100) by Plasma-Assisted Atomic Layer Deposition.

K. Black,[†] M. Werner,[‡] R. Rowlands−Jones,[†] P.R. Chalker,[‡] and M.J. Rosseinsky*[,†]

[†]Department of Chemistry, University of Liverpool, Liverpool L69 3ZD, United Kingdom

[‡]Department of Engineering, Materials Science and Engineering, University of Liverpool, Liverpool L69 3GH, United Kingdom

KEYWORDS: ALD, plasma-assisted, thin film and high-κ dielectric

The scaling down of metal-oxide-semiconductor (MOS) devices beyond the 32 nm node requires a reduced gate dielectric thickness to maintain sufficient capacitance density. This is essential to avoid direct electron tunneling effects and minimize detrimental leakage currents. The use of high-κ dielectric materials with a permittivity that is larger than that of SiO_2, allows an equivalent capacitance density to be achieved in a physically thicker insulating layer (~1 nm).[1] Consequently, there has been a major recent research effort aimed at replacing the existing silicon oxide-based gate dielectric, with alternative high-κ dielectric oxides deposited on Si. Several studies have shown that the perovskite strontium hafnate ($SrHfO_3$) is a promising candidate due to its good physical and electrical properties.[2,3] However, the previous reports of $SrHfO_3$ thin film deposition have been based on MBE, PVD or CVD.[3−5] During the past decade the microelectronics and nanotechnology industry has moved to atomic layer deposition (ALD) for the fabrication of thin film high-κ dielectrics.[6] This is because ALD is capable of coating high-aspect ratio (>60:1) DRAM structures and CMOS dielectrics with very thin, high quality, conformal coatings. ALD meets these requirements due to its saturative, layer-by-layer growth nature and better step coverage compared to other thin film deposition techniques. $SrHfO_3$ films have not previously been deposited by ALD. Previous research on the deposition of $SrZrO_3$ by metallorganic CVD and sol gel methods have highlighted problems associated with achieving stoichiometric compositions.[7]

The deposition of strontium titanate ($SrTiO_3$) has, however, been extensively investigated using ALD. For example, $Sr(^tBu_3Cp)_2$ has been used with water vapor as the oxidant.[7] It was observed that shorter pulse durations of water vapor were required for $SrTiO_3$ in comparison to the direct growth of TiO_2. This was attributed to higher concentrations of hydroxyl groups after the hydrolysis of the Sr precursor. Although SrO is stable in a vacuum or an inert gas environment, it easily hydroxylates in the presence of water. An analogous situation has been observed for $BaTiO_3$ growth. When water is used as the coreagent in the ALD process, it was found that unless extremely long purge times are used, $Ba(OH)_2$ is always deposited.[8,9]

Initially, $Sr(^tBu_3Cp)_2$ was investigated as a strontium source, using water vapor as the oxidant for the growth of $SrHfO_3$. The deposition of strontium hafnate on Si(100) was attempted using ALD cycles of $Sr(^tBu_3Cp)_2/H_2O$ and $(MeCp)_2Hf(OMe)Me/H_2O$. The pulse length of the strontium dose was varied systematically up to 30 s in duration, in order to control the Sr:Hf ratio.

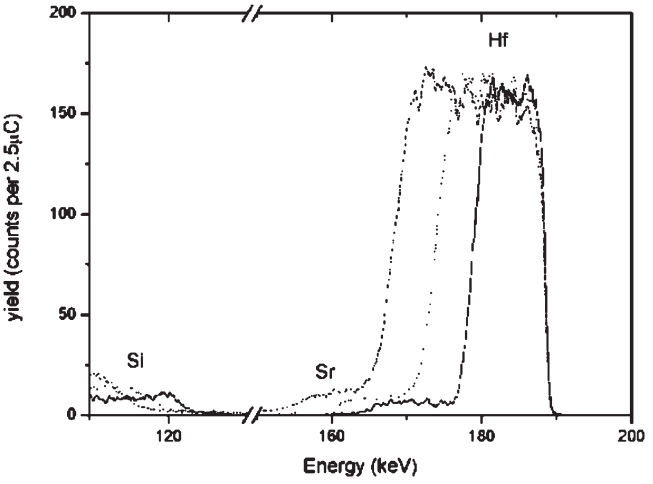

Figure 1. Medium energy ion scattering energy profiles showing the elemental contributions of Sr and Hf in films grown using 10 (—), 20 (· · · ·), and 30s (· − ·)pulses of $Sr(^tBu_3Cp)_2$.

The thickness and composition of films deposited at 300 °C were assessed using medium energy ion scattering (MEIS).[10] Figure 1 shows the energy spectrum of the hafnium and strontium contents of three $Sr_xHf_{1-x}O_2$ films recorded at a scattering angle of 125.3° to collect ions emerging from the ⟨100⟩ direction perpendicular to the Si(100) face. Under these conditions the Sr and Hf content of the films can be effectively mass-separated. Under saturative dosing conditions, increasing the Sr precursor pulse length has little effect on the strontium content. Unexpectedly however the deposition rate and consequently, the thickness of the films, increases dramatically. This could be attributed to an adverse reaction between the Sr layers with water vapor, which causes excessive subsequent hafnium oxide deposition.

To establish whether the enhanced Hf incorporation was due to the $Sr(^tBu_3Cp)_2$ precursor itself or more generically the SrO layer, the use of an alternative precursor namely $Sr(^iPr_3Cp)_2$, was explored. To address the issues of whether the effect of water caused the hafnium enhancement, a comparison was made using an oxygen plasma as an alternative oxidant. A maximum deposition rate per ALD growth cycle was observed at a substrate

Received: January 31, 2011
Revised: March 21, 2011
Published: April 26, 2011

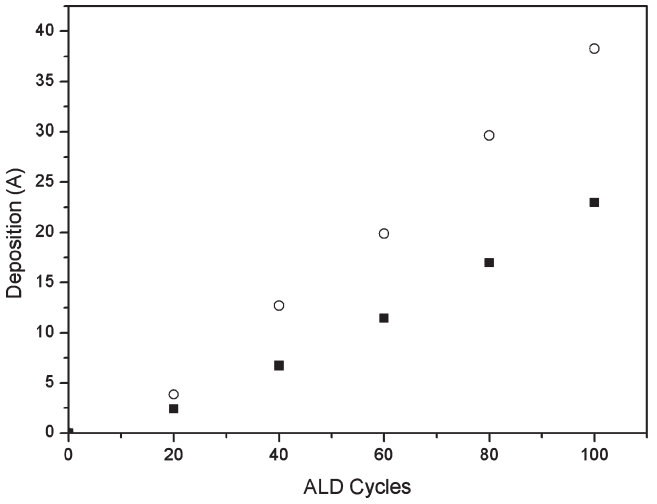

Figure 2. Deposition rate of SrO from $Sr(^{i}PrCp)_2$ with O_2 plasma (○) and water (■) oxidants as a function of the number of ALD cycles at 250 °C.

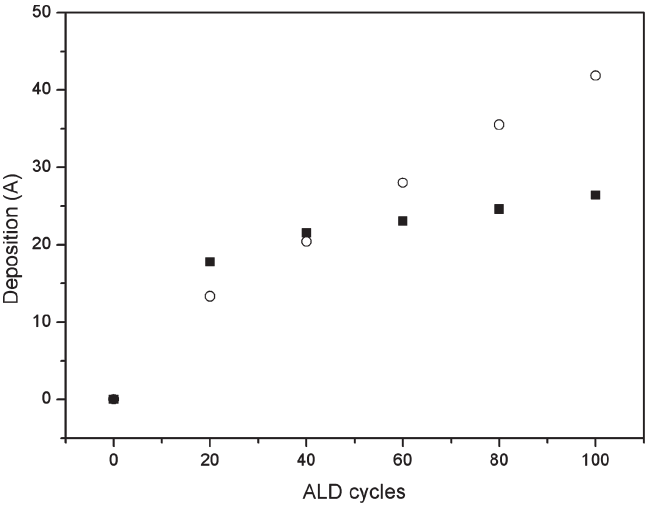

Figure 3. Growth rates of HfO_2 on 40 Å SrO layers using ○ O_2 plasma and ■ water.

temperature of 250 °C. The deposition rate of SrO was explored using in situ spectroscopic ellipsometry. Figure 2 shows the growth rate as a function of ALD cycles for the deposition of SrO using the $Sr(^{i}Pr_3Cp)_2$ with cyclic exposure to an oxygen plasma (300W, 3s) compared with water vapor (0.02s).

Figure 2 shows a characteristic linear relationship between the deposition and the number of ALD cycles with a growth rate of ~0.39 Å/cycle for the oxygen plasma. This is consistent with a saturative growth mode.[11] If water vapor is used instead, a lower growth rate (~0.23 Å/cycle) is observed. These data were used to predeposit two ~40 Å thick SrO layers using either the oxygen plasma or water vapor as oxidants. Without exposing these to atmosphere, the SrO films were overgrown with HfO_2 ($(MeCp)_2Hf$ (OMe)Me) using the same oxygen sources. $(MeCp)_2Hf(OMe)Me$ does not usually deposit at 250 °C when using water as the oxidant. However it can be seen from Figure 3 that the deposition of HfO_2 with water shows a rapid initial growth rate, followed by a subsequent leveling-off. This is attributed to the consumption of the hydroxyl groups in the Sr layer by the Hf source, followed by a rapid decline in growth rate. This decline in growth is due to the exhaustion of the source of reactive hydroxyl groups. By contrast, the Hf grown with the oxygen plasma on an oxygen plasma SrO film, exhibits a linear relationship with the number of ALD cycles. This linearity allows greater contol over the deposition rate required to form the ternary oxide phase. On the basis of these observations, we have developed a plasma-assisted ALD process to enable the deposition of stoichiometric $SrHfO_3$.

Herein, we demonstrate the deposition of $SrHfO_3$ films by oxygen plasma-assisted ALD, on Si(100) substrates to explore the relationship between its crystalline phase and permittivity. The deposition of $SrHfO_3$ films is investigated at a substrate temperature of 250 °C using a Oxford Instruments Opal Reactor. A growth temperature of 250 °C was chosen as the optimum for matching the deposition rates of SrO and HfO_2. The metal precursors used were $Sr(^{i}Pr_3Cp)_2$ and $(MeCp)_2Hf$ (OMe)Me with an oxygen plasma as the oxidant. The plasma was generated using a 300W power source, a frequency of 13.56 MHz, 60 sccm of O_2 and 10 sccm of Ar. The Sr and Hf sources were evaporated at 120 and 100 °C, respectively. An argon carrier gas flow rate of

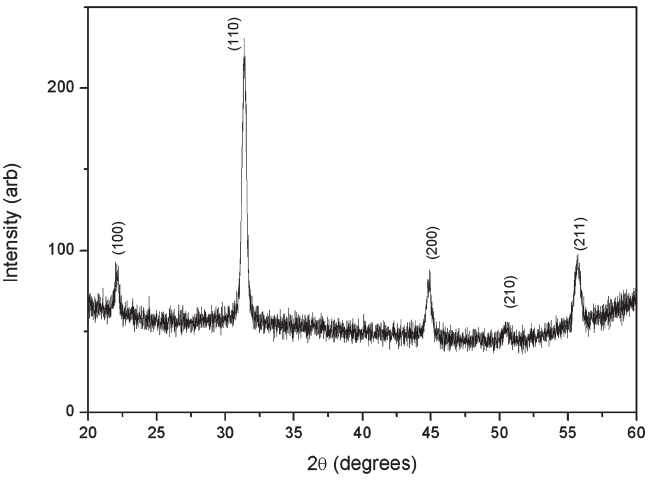

Figure 4. X-ray diffraction pattern of a $SrHfO_3$ film grown from a 3:1 Sr:Hf deposition ratio annealed in air at 600 °C for 30 min.

200 cm^3 min^{-1} was used with a reactor pressure of 5 mbar. The number of ALD cycles was in the range of 50−150, yielding film thicknesses of 15−57 nm. The [precursor/purge/oxidant/purge/−] pulse sequences were n[Sr10s/5s/0.02s/5s] and m[Hf 3s/5s/0.02s/5s] (where n and m were varied depending on the desired Sr:Hf ratio). The different precursor ratios used were: 3:1, 3:2, 5:2, and 7:2. Samples were prepared as thin sections so that energy-dispersive X-ray analysis could be carried out and this showed that for films deposited with a 3:1 (Sr:Hf) cycle ratio a Sr:Hf composition of 1:1 was observed. The other ratios resulted in non stoichometric films. The need for a 3:1 ratio is attributed to the faster growth rate of HfO_2 using $(MeCp)_2Hf(OMe)Me$ than for SrO employing the $Sr(iPr_3Cp)_2$ source.

Films deposited using the 3:1 Sr:Hf ratio were selected for subsequent physicochemical and electrical characterization. X-ray diffraction analysis of a film grown at 250 °C by ALD (not shown) did not reveal any diffraction features, indicating that it was essentially amorphous as deposited. Figure 4 shows that, after annealing in air at 600 °C for 30 min, the film showed

dx.doi.org/10.1021/cm200315u |*Chem. Mater.* 2011, 23, 2518–2520

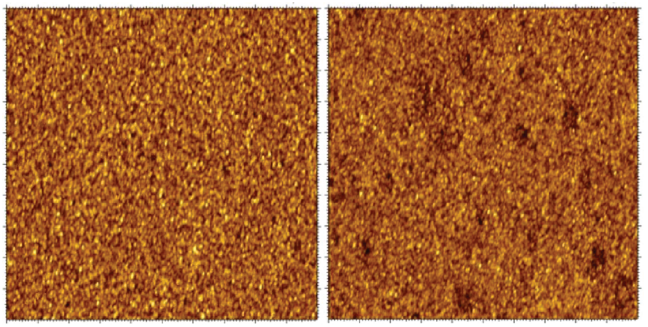

Figure 5. Atomic force micrograph of: left, as deposited $SrHfO_3$ film; right, film after annealing in air at 600 °C for 30 min.

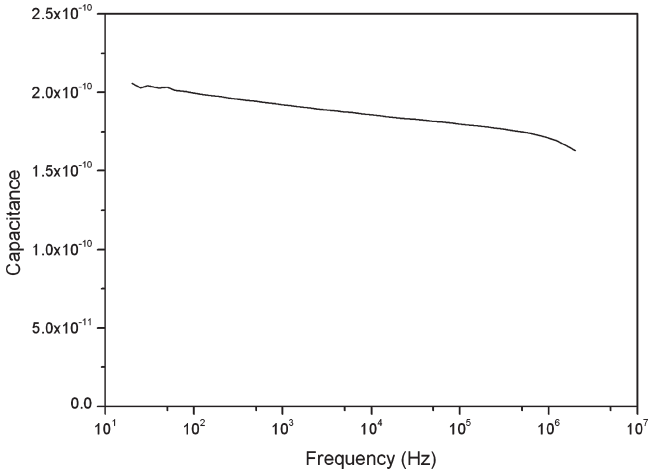

Figure 6. Capacitance dispersion of a $SrHfO_3$ MOS capacitor as a function of frequency.

diffraction features that correspond to either the cubic or orthorhombic phase of $SrHfO_3$. These phases are indistiguishable for the thin films investigated here using XRD. The c-lattice constant of the $SrHfO_3$ films determined by XRD is 4.06 Å. This is in agreement with the structural parameters obtained for bulk $SrHfO_3$ (cubic, $Pm3m$ a = 4.08 Å)[12]

Atomic force microscopy (Figure 5) shows that the $SrHfO_3$ films deposited, after annealing in air, are smooth with a root-mean-square (rms) roughness of 7.0 Å over a 5 × 5 μm^2 area. The darker areas of contrast that appear after annealing accompany the crystallization process, but represents a roughening of approximately only 1 Å peak-to-valley for a film thickness of 57 nm.

The retention of a smooth morphology is a significant advantage for dielectrics used in MOS gate-stack applications. Metal-oxide-semiconductor (MOS) capacitors were fabricated to assess the dielectric properties of the $SrHfO_3$ films after air annealing at 600 °C. The performance of MOS field effect transistors can be significantly impaired by dielectric relaxation effects. This is a potential issue for most crystalline, high-κ dielectrics compared with SiO_2. Capacitance−frequency (C−f) data from a typical MOS capacitor [Au/$SrHfO_3$/Si/Al] are shown in Figure 6. The $SrHfO_2$ film thickness of 57 nm was chosen to minimize the contribution from an SiO_2 interlayer. The C−f data show a shallow frequency dispersion without any low-frequency (<1 kHz) "sheathlike" grain boundary contributions.[13] A relative permittivity (κ) of 21 was extracted from the accumulation capacitance at 100 kHz. This was derived after accounting for the presence of a 3.2 nm SiO_2 interlayer as quantified by X-ray reflectivity and ellipsometery. The thickness of the interlayer is attributed to the affects of annealing in air. This permittivity value is in close agreement with $SrHfO_3$ films deposited on Si by alternative deposition techniques, such as MBE.[2]

In summary, stoichiometric strontium hafnate thin films have successfully been deposited by employing plasma-assisted ALD. The film composition can be controlled by altering the Sr:Hf ratio by varying the relative numbers of cycles of strontium and hafnium deposition. Perovskite structure $SrHfO_3$ films crystallized after annealing at 600 °C. The crystalline $SrHfO_3$ dielectric has a relative permittivity (κ) of 21 measured at a 100 kHz bias voltage. The high permittivity and low frequency dispersion of the strontium hafnate films make them candidates for the next generation of high-κ based semiconductor devices.

■ ACKNOWLEDGMENT

We acknowledge the financial support of the Engineering and Physical Sciences research council (EPSRC) through the Knowledge Transfer Initiative (EPSRC EP/H500146/1) and the Northwest Development Agency through the Knowledge Centre for Materials Chemistry (KCMC).

■ REFERENCES

(1) International Technology Roadmap for Semiconductors 2009; http://www.itrs.net/links/2009ITRS/Home2009.htm

(2) Sousa, M.; Rossel, C.; Marchiori, C.; Siegwart, H.; Caimi, D.; Locquet, J. P.; Webb, D. J.; Germann, R.; Fompeyrine., J. *J. Appl. Phys.* **2007**, *102*, 104103.

(3) Rossel, C.; Mereu, B.; Marchiori, C.; Caimi, D.; Sousa, M.; Guiller, A.; Siegwart, H.; Germann, R.; Locquet, J. P.; Fompeyrine, J.; Webb, D. J. *Appl. Phys. Lett.* **2006**, *89*, 053506.

(4) McCarth, I.; Agustin, M. P.; Shamuilia, S .; Stemmer, S.; Afanas'ev, V. V.; Campbell, S. A. *Thin Solid Films* **2006**, *515* (4), 2527–2530.

(5) Luo, B.; Yu, D.; Kucera, B. E.; Campbell, S. A.; Gladfelter, W. L. *Chemical Vapor Deposition* **2007**, *13* (8), 381–388.

(6) S. De Gendt, Bent, S. F.; Delabie, A.; Elam, J. W.; Kang, S. B.; O. van der Straten, L. A. *Atomic Layer Deposition Applications 5*; Vienna, Austria, October 4−9, 2009; ECS Transactions; The Electrochemical Society: Pennington, NJ, 2009; Vol. 25, Issue 4.

(7) Andrieux, M.; Gasquéres, C.; Legros, C.; Gallet, I.; Herbst-Ghysel, M.; Condat, M.; Kessler, V. G.; Seisenbaeva, G. A.; Heintz, O.; Poissonnet, S. *Appl. Surf. Sci.* **2007**, *253*, 9091–9098.

(8) Vehkamäki, M.; Hanninen, T.; Ritala, M.; Leskelä, M.; Sajavaara, T.; Rauhala, E.; Keinonen, J. *J. Chem. Vapor Deposition* **2001**, *7* (2), 75–80.

(9) Vehkamäki, M.; Hatanpää, T.; Ritala, M.; Leskelä, M.; Väyrynen, S.; Rauhala, E. *J. Chem. Vapor Deposition* **2007**, *13*, 239–246.

(10) Bailey, P.; Noakes, T. C. Q.; Woodruff, D. P. *Surf. Sci.* **1999**, *426*, 358.

(11) Niinistö, L.; Päiväsaari, J.; Niinistö, J.; Putkonen, M.; Nieminen, M. *Phys. Status Solidi A* **2004**, *201* (No. 7), 1443–1452.

(12) Yamanaka, S.; Maekawa, T.; Muta, H.; Matsuda, T.; Kobayashi, S.-i.; Kurosaki, K. *J. Solid State Chem.* **2004**, *177*, 3484–3489.

(13) Zhao, C. Z.; Taylor, S.; Werner, M.; Chalker, P. R.; Gaskell, J. M.; Jones, A. C. *J. Vac. Sci. Technol., B* **2009**, *27* (1), 333–337.